Development of a 2D full-wave JE-FDTD Maxwell X-mode code for reflectometry simulation

F. da Silva, [†]S. Heuraux, [§‡]T. Ribeiro and [‡]B. Scott

[§]*Associação EURATOM/IST–Instituto de Plasmas e Fusão*
Instituto Superior Técnico, 1046-001 Lisboa, Portugal

[†]*IJL Nancy-Université*
CNRS UMR 7198, BP 70239, F-54506 Vandœuvre Cedex, France

[‡] *Max-Planck-Institut für Plasmaphysik*
EURATOM Association, Garching, Germany

Abstract

A 2D full-wave FDTD code is being developed and integrated with the output of a state-of-the-art turbulence code implementing a complete synthetic diagnostic capable of coping with the complex signature of turbulence. The turbulence code used is a gyrofluid electromagnetic model with global geometry (GEMR). The X-mode wave-propagation code solves Maxwell equations using a finite-difference time-domain technique coupled to the ordinary differential equations of the motion or to differential equations describing the plasma behaviour. The plasma current equation is handled through a novel solver (JE) that allows a fast direct FDTD implementation which constitutes an improvement over the much slower Runge-Kutta solvers, traditionally used.

1 Introduction

An important tool for the progress of reflectometry is numerical simulation, able to assess the measuring capabilities of existing systems and to predict the performance of future ones in machines such as ITER and DEMO. To simulate X-mode reflectometry in a comprehensive set of plasmas scenarios and experiments, a two-dimensional (2D) full-wave finite-differences time-domain (FDTD) code is being developed and integrated with the output of a state-of-the-art turbulence code, implementing a complete synthetic diagnostic capable of coping with the complex signature of turbulence. The turbulence code used is a six moments gyrofluid electromagnetic model with global geometry (GEMR) [1], [2]. The X-mode wave-propagation code solves Maxwell equations using a FDTD technique coupled to the ordinary differential equations of the motion or to differential equations describing the plasma behaviour. The plasma current equation is handled through a novel solver (JE) [3] that allows a direct FDTD implementation, which constitutes an improvement over the much slower Runge-Kutta solvers, traditionally used. Such numerical scheme can be used to develop a 3D code including collision effects. The main characteristics of the X-mode code are presented together with a description of its integration with the turbulence code. This approach to a synthetic diagnostic will provide a better understanding of the complexity associated with reflectometry measurements.

2 REFMULX—The X-mode code

The need to simulate X-mode reflectometry led to the development of a 2D full-wave Maxwell FDTD, REFMULX. This code complements the available O-mode code (REFMUL) drawing upon the experience gained during REFMUL's implementation, being an example, the rewriting of the unidirectional transparent

source (UTS) [4] for X-mode. To better design a synthetic diagnostic the code has the possibility of include, as plasma models, the results calculated by external codes which provide a more thorough description of the plasma behaviour than the simpler internal models native to REFMULX. Internal models can be used when a simplified description is needed to simulate a certain plasma behaviour (e.g. to isolate forward scattering response without any Bragg backscattering) or to test an hypothesis in a controlled plasma scenario, while the external plasma input would spring into action when a more close to reality scenario is envisaged. In the code the plasma is considered stationary on wave-time reference ($\tau_{plasma} \gg T_{wav}$), ions are considered motionless (ion cyclotron frequency $\omega_{ci} \ll \omega_{wav}$) and thermal electron velocity smaller than phase velocity ($v_{th} \ll v_{ph}$). We assume a transversal electric (TE), i.e. X-mode propagation (wave magnetic field $\mathbf{H} \parallel \mathbf{B_0}$) in a 2D plane ($x$–$y$) perpendicular to which a static magnetic field is set ($\mathbf{B_0}$) and no gradients are admitted along this axis ($\partial/\partial z = 0$). With this considerations, Maxwell curl equations appear as a simpler set of differential equations

$$\begin{aligned} \varepsilon_0 \frac{\partial E_x}{\partial t} + \sigma E_x &= \frac{\partial H_z}{\partial y} - J_x \\ \varepsilon_0 \frac{\partial E_y}{\partial t} + \sigma E_y &= -\frac{\partial H_z}{\partial x} - J_y \\ \mu_0 \frac{\partial H_z}{\partial t} + \sigma^\star H_z &= \frac{\partial E_x}{\partial y} - \frac{\partial E_y}{\partial x}, \end{aligned} \tag{1}$$

where $\sigma E_{x,y}$ and $\sigma^\star H_z$ are responsible for the implementation of a perfectly matched layer (PML) [5]. The plasma is handled by the current density $J_{x,y}$. This set of PDEs will be solved using FDTD with the classical Yee algorithm [6]. More details on its implementation can be found in [7], [8]. Metallic conditions is set using a numeric perfectly magnetic conductor condition [7]. To couple the propagation equations to the plasma the equation of movement

$$\frac{\mathrm{d}\mathbf{J}}{\mathrm{d}t} = \varepsilon_0 \omega_p^2 \mathbf{E} - \nu \mathbf{J} + \omega_c \hat{\mathbf{b}} \times \mathbf{J}, \tag{2}$$

must be solved at each time-step, where $\hat{\mathbf{b}}$ represents the direction along the magnetic field. This is usually the most delicate part when solving this kind of codes since an algorithm which is stable and efficient must be found. We resort here to one proposed by Xu and Yuan [3] which fulfills these requirements. For 2D without collisions ($\nu = 0$) solving $\mathbf{J}$ is reduced to

$$\begin{aligned} J_x^{n+1/2} &= \frac{1 - \frac{\omega_c^2 \Delta t^2}{4}}{1 + \frac{\omega_c^2 \Delta t^2}{4}} J_x^{n-1/2} - \frac{\omega_c \Delta t}{1 + \frac{\omega_c^2 \Delta t^2}{4}} J_y^{n-1/2} + \frac{\varepsilon_0 \omega_p^2 \Delta t}{1 + \frac{\omega_c^2 \Delta t^2}{4}} \left(E_x^n - \frac{\omega_c \Delta t}{2} E_y^n \right) \\ J_y^{n+1/2} &= \frac{1 - \frac{\omega_c^2 \Delta t^2}{4}}{1 + \frac{\omega_c^2 \Delta t^2}{4}} J_y^{n-1/2} + \frac{\omega_c \Delta t}{1 + \frac{\omega_c^2 \Delta t^2}{4}} J_x^{n-1/2} + \frac{\varepsilon_0 \omega_p^2 \Delta t}{1 + \frac{\omega_c^2 \Delta t^2}{4}} \left(E_y^n + \frac{\omega_c \Delta t}{2} E_x^n \right). \end{aligned} \tag{3}$$

This is quite efficient when compared with Runge-Kuta of 4th order (RK4), a technique traditionally used to solve this problem. With this new schema only 5 equations, 3 for $\mathbf{H}$ and $\mathbf{E}$ and 2 for $\mathbf{J}$, have to be solved. Compare it to RK4 where 10 equations are needed for $\mathbf{J}$, and since these use all values of $\mathbf{H}$ and $\mathbf{E}$ at every half iteration, one has to solve two systems shifted of $n/2$, adding to a grand total of 16 equations.

Plasma density $n_e(\mathrm{r}, t)$ is introduced in the definition of $\omega_p^2 = n_e e^2/\varepsilon_0 m_e$ and the external magnetic field $B_0(\mathrm{r}, t)$ through $\omega_c = eB_0/m_e$. In this work they are given by an external code, GEMR.

3 GEMR

The density fluctuations are computed by means of a three dimensional electromagnetic gyrofluid model with global geometry. This model is derived by taking the first six moments of the gyrokinetic equation, namely, densities, parallel velocities, parallel and perpendicular temperatures and parallel heat fluxes associated with each temperature, all for each plasma species [9], and using a consistent treatment of the energy conservation [1]. The extra equations necessary to yield a closed system are the ones that rule the fields, namely, the gyrokinetic polarisation equation for the electrostatic potential [10], and the Ampère's law for the parallel magnetic vector potential, since the model is electromagnetic. The latter property together with the fact that not only the fluctuations but also the background profiles are evolved in time implies that a dynamical Shafranov shift and a correction to the magnetic field pitch are calculated and treated self consistently in the model [11]. The geometry is global in the sense that the radial dependence of the geometrical quantities is kept (no flux tube approximation made). The coordinates used are field aligned, and hence non-orthogonal, due to the computational efficiency gain they allow in magnetised plasmas, where a strong spatial anisotropy between the direction along the magnetic field, and the plane perpendicular to it exists. The choice is to have one coordinate (s) aligned with the magnetic field, and the remaining (x and y) perpendicular to it, such that only one contravariant component of the magnetic field is finite ($\mathbf{B}\cdot\nabla s = B^s$), with the remaining two vanishing ($\mathbf{B}\cdot\nabla x = \mathbf{B}\cdot\nabla y = 0$) [12]. To avoid confusion it is noteworthy that the coordinates x, y are different from their counter parts in REFMULX. Since the goal is to probe the plasma electron density with reflectometry on the poloidal plane, post processing coordinates transformations from the field aligned GEMR coordinate system (x, y, s) to the usual cylindrical coordinate system (x, θ, ϕ) has to be done. This involved transforming into Fourier space in the GEMR toroidal angle coordinate (y) to apply a phase shift that undoes the shifted metric procedure [13]. An interpolation from the typical low resolution parallel grid to an high resolution one follows, after which a phase factor of q (magnetic field pitch) is applied to transform back to an unaligned representation, that is to move from a parallel coordinate s to a poloidal one θ. To finalise, an inverse Fourier transform is applied by summing the transformed toroidal Fourier modes, which yields a single poloidal plane, where the data to provide to the REFMULX code, namely, n_e and B_0 are then measured.

The preliminary GEMR simulations performed here served as a proof of principle for our synthetic reflectometer diagnostic. They assumed a simplified circular magnetic equilibrium with local plasma parameters representative of a typical ASDEX Upgrade (AUG) L-mode discharge, namely,

$$T_i = T_e = 100\,\mathrm{eV}, \qquad n_i = n_e = 2.0\times10^{19}\mathrm{m}^{-3}$$

$$M_D = 3670\,m_e, \qquad Z_{eff} = 2, \qquad B = 2.0\,\mathrm{T}, \qquad q = 3.5$$

$$R = 1.65\,\mathrm{m}, \qquad a = 0.5\,\mathrm{m}, \qquad L_T = L_n/2 = 3.5\,\mathrm{cm}$$

The radial domain includes both edge and scrape-off layer (SOL) regions. It should be noted that the continuation of this work is foreseen and will involve using better resolved (larger) turbulence simulations, some of which are already under way, as well as simulations using realistic AUG geometry.

4 Codes integration

Although simulating the same reality, different codes use distinct models and mathematical descriptions of that same reality, and a direct coupling between them is more often than not impossible. Some work has to be done to integrate them and this is true for REFMULX and GEMR. First, a standard for the data to share between the codes is to be decided upon. We chose to use the HDF5 format, since it widely used in tokamak turbulence models nowadays.

The time discretization of GEMR is usually much larger than the one used in REFMULX. As a start point for these simulations we have considered the plasma frozen in the time frame of the probing signal. GEMR

provides poloidal cuts of the plasma defined on a polar geometry (r, θ) while REFMULX uses a Cartesian one, (x, y). The points of the two meshes do not, obviously, coincide. Furthermore, the points of the polar grid are not equidistantly distributed, a fact that lead us to treat the problem with the tools usual to problems of unregular meshes. One of these techniques is Delaunay interpolation and we used it to interpolate the GEMR's plasma description into the REFMULX's one with the needed spatial resolution of $20\,\mathrm{points}/\lambda$. To note that the corner of the Cartesian grids correspond to spatial positions not included in the polar grid to which a value must be given. They correspond however to positions in a vacuum and are set to null density.

A similar interpolation procedure is done for the external magnetic field B_0, also provided by GEMR. The interpolation is not performed on all the poloidal cut but only in the a region of interest (ROI) for the simulation, in this work, the equatorial low-field side (LFS).

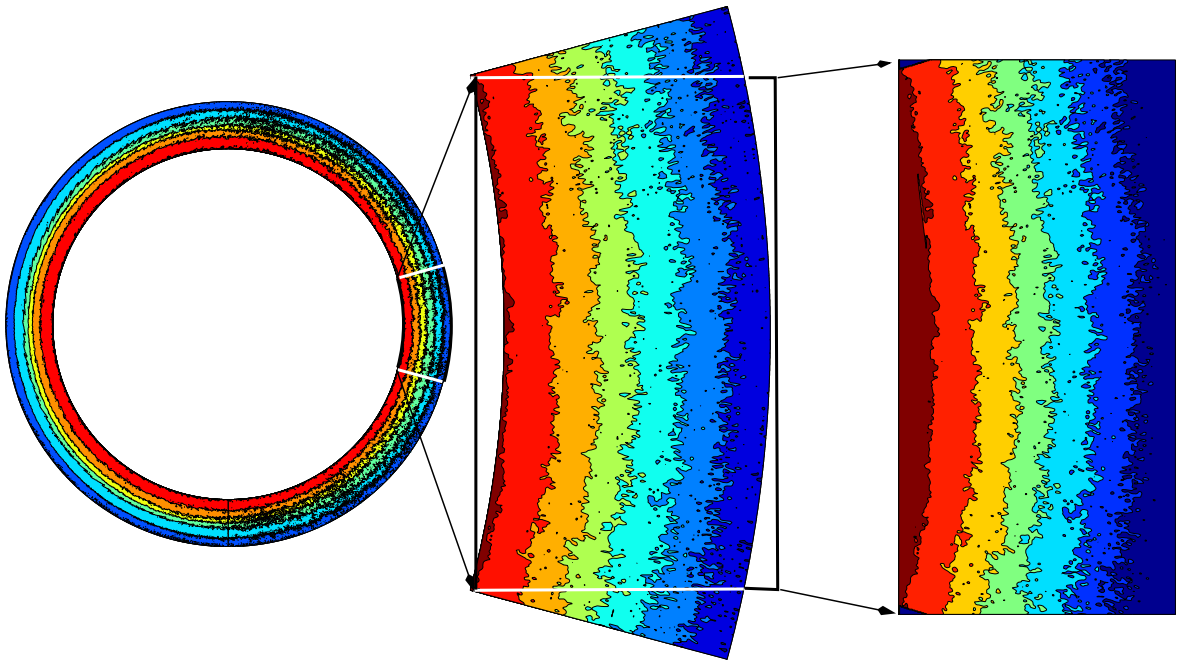

Figure 1: GEMR provides a poloidal cut of the plasma defined on a polar geometry (r, θ) (left). Only a section of the poloidal cut is region of interest (ROI) for the simulation (center) and is Delauney interpolated into a rectangular Cartesian region (right).

5 Simulations and results

With the provided density and magnetic field a frequency sweep simulation was done with the plasma being probed in the band Ka, 30–40 GHz. A field contour snapshot is presented in Fig. 2—top left. The field detected in the waveguide, decoupled from the stronger main emission due to the use of an UTS, is processed using a in-phase/quadrature (I/Q) detection. The resulting signals appear in Fig. 2—top right. They exhibit a low frequency trend, amplitude modulation and some low amplitude high frequency components. Using simple signal processing tools (polynomial detrend, low pass filtering and amplitude normalization) a pair of *clean* I/Q normalized signals is obtained which can be used to get the phase $\varphi(f)$ and from it the phase derivative $\partial\varphi/\partial f$, one of the key ingredients for a profile evaluation. Another possible technique is to use a sliding fast Fourier transform (SFFT) on one of the I/Q signals to get the beat frequency f_B of the signal and from it the phase derivative $\partial\varphi/\partial f = 2\pi f_B(\partial f/\partial t)^{-1}$. The SFFT of the In-phase signal is show in Fig. 2—bottom left. The phase derivatives obtained using these two techniques appear on Fig. 2—bottom right with the blue curve showing the SFFT result and the red curve the I/Q one.

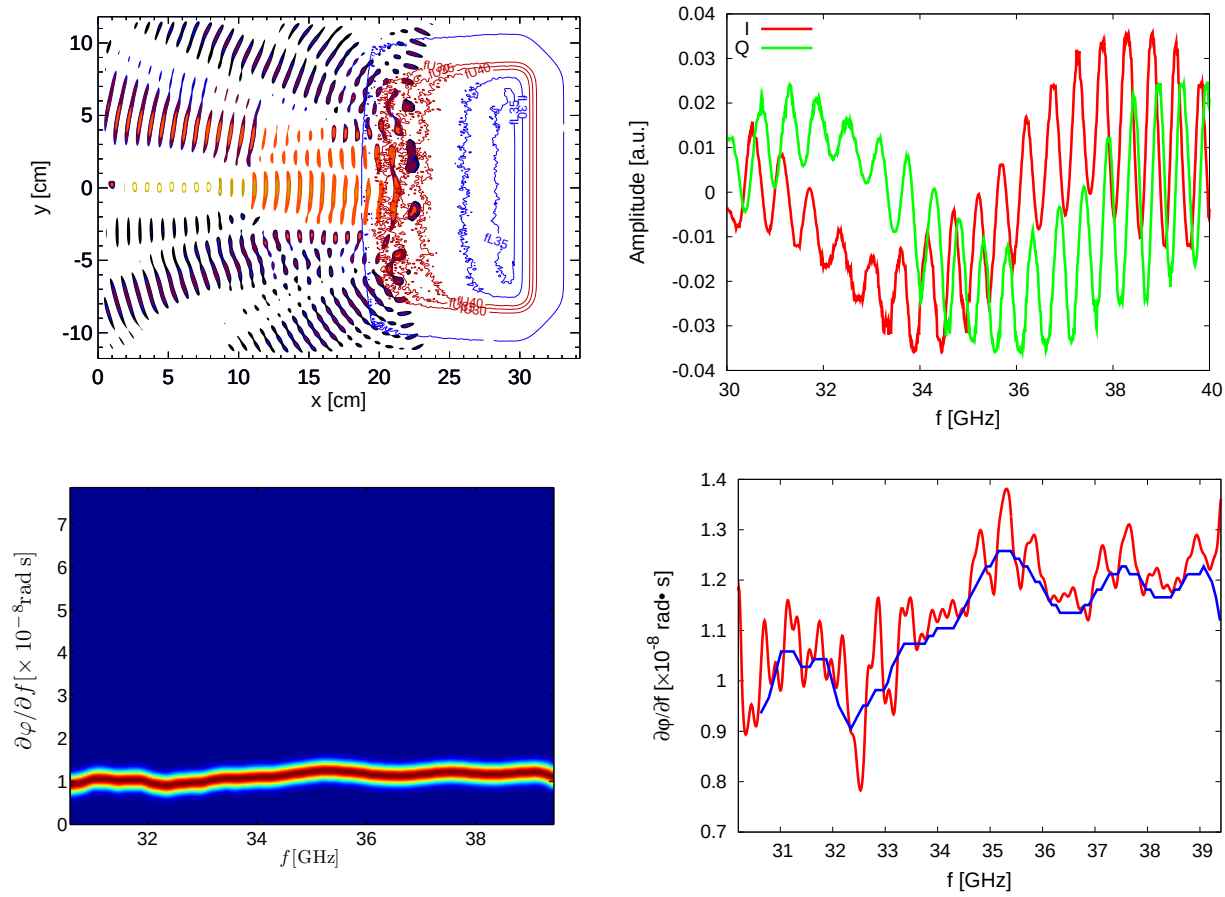

Figure 2: A field contour snapshot of the simulation(top left). Detected I/Q signals (top right). The SFFT of the In-phase signal (bottom left). The phase derivatives obtained with a SFFT of the in-phase signal (blue) and with I/Q deconvolution (red) (bottom right).

Acknowledgements

This work, supported by the European Communities and *Instituto Superior Técnico*, has been carried out within the Contract of Association between EURATOM and IST. Financial support was also received from *Fundação para a Ciência e Tecnologia* in the frame of the Contract of Associated Laboratory. The views and opinions expressed herein do not necessarily reflect those of the European Commission, IST and FCT.

References

[1] B. Scott. *Physic of Plasmas*, 12:p102307, 2005

[2] B. Scott and R. Hatzky. *35th EPS Conf. on Plasma Phys. Hersonissos*, 9-13 June 2008 ECA, Vol.32D, P-5.031, 2008.

[3] L. Xu and N. Yuan. *IEEE antennas and wireless propagation letters*, 5:335–338, 2006.

[4] F. da Silva, S. Heuraux, S. Hacquin, and M. Manso. *Journal of Computational Physics*, 203(2):467–492, 2005.

[5] Jean-Pierre Berenger. *Journal of Computational Physics*, 114(2):185–200, 1994.

[6] K. S. Yee. *IEEE Transactions on Antennas and Propagation*, 14:302–307, 1966.

[7] Allen Taflove and Susan C. Hagness. *Computational Electrodynamics: The Finite-Difference Time-Domain Method, Second Edition*.

[8] K.S.Kunz, R.J.Luebbers. *The finite difference time domain method for electromagnetism*.

[9] M. A. Beer and G. Hammett. *Phys. Plasmas*, 3:4046, 1996.

[10] W. W. Lee. *Phys. Fluids*, 26:556, 1983.

[11] B. Scott. *Contrib. Plasma Phys.*, 46:714, 2006

[12] R. L. Dewar and A. H. Glasser. *Phys. Fluids*, 26:3038, 1983.

[13] B. Scott. *Phys. Plasmas*, 8:447, 2001.